

Scaling behavior in InAs/GaAs(001) quantum-dot formation

T. J. Krzyzewski, P. B. Joyce, G. R. Bell, and T. S. Jones*

Centre for Electronic Materials and Devices, Department of Chemistry, Imperial College of Science, Technology and Medicine,
London SW7 2AY, United Kingdom

(Received 3 September 2002; published 26 November 2002)

Scanning tunneling microscopy has been used to investigate the nucleation and evolution of InAs/GaAs(001) quantum dots (QD's) grown by molecular beam epitaxy. No scaling behavior as a function of coverage is observed for the QD size distributions during their initial stages of formation. At coverages close to the critical coverage the shape of the QD volume distribution resembles an $i=0$ scaling curve, and a modified $i=1$ curve after saturation of the QD number density, with a crossover regime in between. The results show that strain has a significant influence during QD nucleation and the initial stages of growth, but is unimportant in the later stages of QD development. Comparison with classic nucleation theory indicates a large, temperature-dependent size for the critical nucleus ($i=18$ at 500 °C). This disagrees with conventional models of QD formation and highlights the limited applicability of simple growth theories in modeling complex heteroepitaxial growth systems.

DOI: 10.1103/PhysRevB.66.201302

PACS number(s): 68.55.Ac, 68.37.Ef, 81.15.Hi

The growth of coherent self-assembled quantum dots (QD's) in lattice-mismatched semiconductor systems such as InAs/GaAs(001) has attracted considerable interest primarily because of their possible uses as the active layer in next-generation optoelectronic devices.¹ The ability to tune the QD properties to specific device requirements depends to a large extent on understanding how factors such as temperature and growth rate affect the QD size distribution. Unfortunately, very important fundamental aspects of InAs/GaAs(001) QD formation remain poorly understood, for example the exact mechanism of the two-dimensional \rightarrow three-dimensional (2D \rightarrow 3D) growth mode transition and subsequent QD development, and the relative importance of thermodynamic versus kinetic effects. Thermodynamic models of QD formation^{2,3,4,5} have been shown to have limited applicability, and attempts to fit experimental data using kinetic (Monte Carlo and rate equation) simulations^{6,7} have been only partially successful.

For simple 2D submonolayer growth, it has been shown from nucleation theory⁸ that the island size distribution obeys a scaling law of the form:⁹

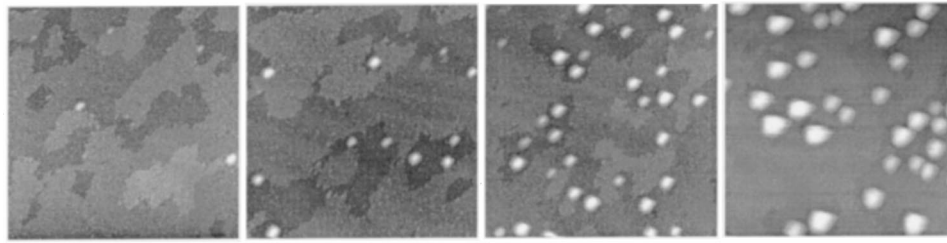
$$N_s = \frac{\theta_{\text{eff}}}{\langle s \rangle^2} f(s/\langle s \rangle), \quad (1)$$

where N_s is the number of islands containing s atoms, θ_{eff} is the effective surface coverage, $\langle s \rangle$ is the average number of atoms in a 2D island, and $f(s/\langle s \rangle)$ is a scaling function which depends only on $s/\langle s \rangle$. For submonolayer InAs heteroepitaxy on GaAs, 2D island size distributions have been shown to exhibit scaling behavior as a function of InAs coverage,¹⁰ growth rate and temperature,¹¹ III:V flux ratio¹² and substrate orientation,¹³ with the scaling functions closely resembling those observed in GaAs(001) homoepitaxy.^{11,12} The main implication of these results is that the 2D nucleation kinetics in this growth system are determined by effects other than strain, the surface reconstruction playing a dominant role. This conclusion is not surprising since it is unlikely that at the submonolayer coverages studied (<0.3

ML), there is a sufficient amount of material on the surface for the strain energy (which is directly proportional to thickness of deposit) to seriously affect the nucleation and growth of 2D islands. Islands can therefore grow in a pseudomorphic, strain-free fashion, despite the very high lattice mismatch between the GaAs substrate and the InAs deposit.

Recently, Ebiko *et al.*^{14,15} extended the scaling analysis to the 3D growth regime in InAs/GaAs(001) QD formation, using *ex situ* atomic force microscopy (AFM) to study the evolution of the 3D islands grown by molecular beam epitaxy (MBE). Scaling as a function of InAs coverage was observed for both island size and separation at growth temperatures <550 °C, the behavior consistent with that observed for a critical nucleus size $i=1$. This was interpreted as evidence for strain being an *insignificant* factor in determining the QD size distribution. However, their study focused on the postnucleation QD growth regime after saturation of the QD number density (N_s). Such a study does not provide information about the initial QD growth mechanism, because the important stages of QD formation occur before N_s saturation; at best it can only aid the understanding of *mature* QD development. In addition, the effects of QD alloying, which are known to occur at the growth rate and temperatures used in their experiments¹⁴ (~ 0.1 ML s^{-1} and 490–550 °C) were neglected, despite strong evidence for significant alloying in both the wetting layer (WL) and the QD's themselves.^{16,17}

In the original scaling model proposed by Bartelt and Evans¹⁸ (structureless point islands with critical nucleus size $i=1$), no distinction is made between 2D and 3D islands. It is reasonable, therefore, to extend 2D scaling arguments to 3D growth analysis, but care must be taken when using 3D island distribution characteristics, such as θ_{eff} , N_s and $s/\langle s \rangle$, in what remain essentially 2D growth models. For example, θ_{eff} is a fractional coverage, and by definition cannot exceed unity. For 3D Stranski-Krastanov (S-K) growth, this must be taken as being equal to the coverage beyond the 2D-3D transition ($\theta - \theta_{\text{crit}}$, where θ_{crit} is the critical coverage for 3D island formation), which is only true if classic S-K growth is



(a) 1.68 ML (b) 1.72 ML (c) 1.81 ML (d) 2.38 ML

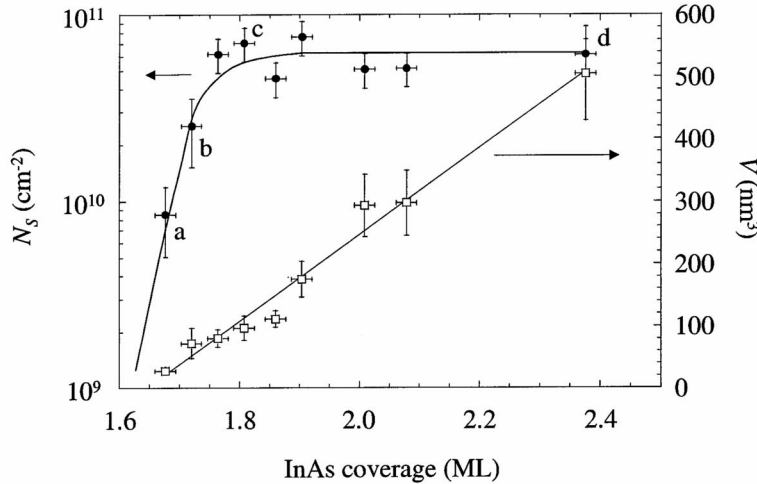


FIG. 1. Filled states STM images ($0.2 \mu\text{m} \times 0.2 \mu\text{m}$) of InAs/GaAs QD formation close to θ_{crit} : (a) $1.68 \text{ ML} = \theta_{\text{crit}} + 0.02 \text{ ML}$, (b) $1.72 \text{ ML} = \theta_{\text{crit}} + 0.06 \text{ ML}$, (c) $1.81 \text{ ML} = \theta_{\text{crit}} + 0.15 \text{ ML}$, (d) $2.38 \text{ ML} = \theta_{\text{crit}} + 0.70 \text{ ML}$. Also shown is a plot of the QD number density N_s (filled circles) and the average QD volume V (empty squares) as a function of InAs coverage. Solid lines are guides to the eye.

assumed and there is no alloying in the WL or QD's. Such assumptions are not always valid, as InAs/GaAs QD's are known to undergo alloying at normal growth temperatures and growth rates.^{16,19} However, we are not concerned with the actual mathematical form of $f(s/\langle s \rangle)$, which is known to

be complicated,⁹ but only its *shape*, and it is sufficient to calculate 3D values for θ_{eff} , N_s , and $s/\langle s \rangle$ in an identical manner to that for 2D islands.

The experimental method has been described in detail elsewhere.^{11,17} Briefly, $\sim 0.1 \mu\text{m}$ GaAs buffer layers were

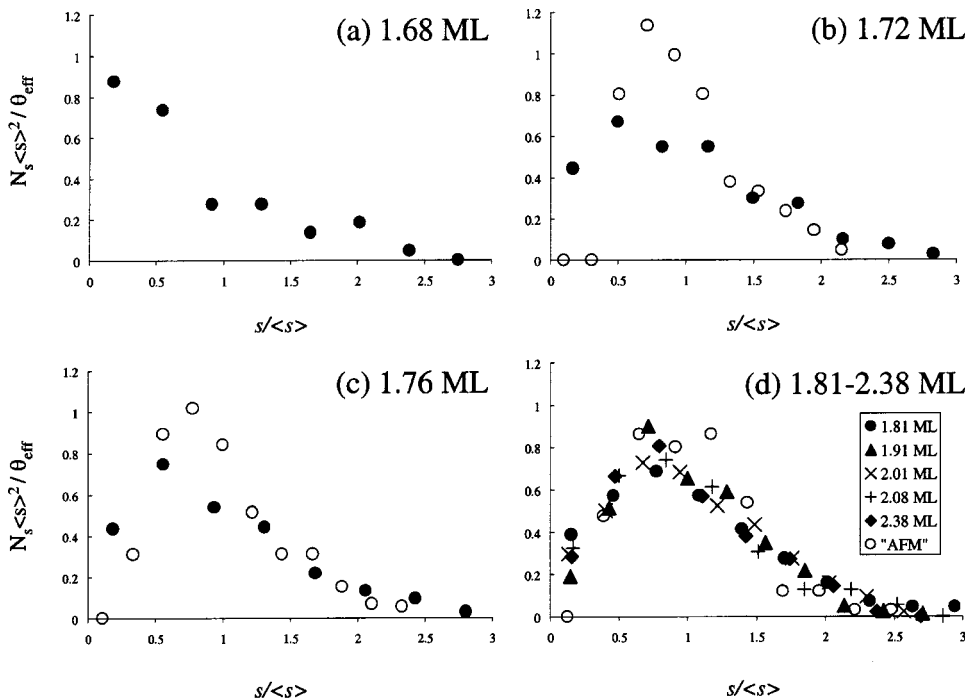


FIG. 2. Scaled QD volume distributions for InAs coverages of: (a) 1.68 ML, (b) 1.72 ML, (c) 1.76 ML, (d) 1.81–2.38 ML. The horizontal ($s/\langle s \rangle$) and vertical ($N_s \langle s \rangle^2 / \theta_{\text{eff}}$) axes are identical for all InAs coverages. Filled symbols refer to conventionally analyzed STM data, empty circles refer to the same data but with the addition of AFM convolution effects.

grown by MBE on nominally flat ($\pm 0.1^\circ$), $n+$ doped, epitaxially GaAs(001) substrates, before deposition of InAs at 0.017 ML s^{-1} ($\pm 2\%$) at a substrate temperature of 490°C . Note that this low growth rate minimizes the alloying in the growth process, and leads to high In content QD's¹⁷; furthermore, it minimizes errors in coverage. For these conditions, θ_{crit} for QD formation is 1.66 ML. All fluxes were calibrated using reflection high-energy electron diffraction (RHEED) intensity oscillations recorded during homoepitaxial growth on GaAs(001) and InAs(001) substrates at 580°C and 400°C , respectively. After completion of growth, the samples were immediately quenched into the adjacent scanning tunneling microscopy (STM) chamber, base pressure $< 1 \times 10^{-10}$ mbar. The rapid transfer time (~ 2 s) and high cooling rate (50°C s^{-1}) ensures the surface morphology is effectively "frozen" and prevents significant postgrowth thermally-induced surface rearrangements. Room-temperature STM images were taken in constant height mode at a bias of -3 to 4 V, with at least two completely different areas of the sample scanned for each coverage.

Figure 1 shows STM images ($0.2 \mu\text{m}^2$) at four InAs coverages corresponding to different stages of InAs/GaAs QD development. Also shown is a plot which shows the variation of QD number density (N_S) and average volume (V) as a function of InAs coverage. In the very earliest stages of QD formation [Fig. 1(a), $\theta = \theta_{\text{crit}} + 0.02 \text{ ML}$] a large number of small 3D islands (height $h = 6 - 12 \text{ \AA}$) nucleate on the surface and N_S increases rapidly. These features develop extremely quickly into larger more mature QD's [Fig. 1(b) $\theta = \theta_{\text{crit}} + 0.06 \text{ ML}$], but as their size increases, the rate at which they grow decreases. The probability of capture of an adatom by an existing 3D island relative to the probability of new nucleation increases; N_S still increases, but more slowly. Eventually, almost all the material available on the surface is incorporated into the QD's and the probability of a new QD nucleating tends to zero. This leads to saturation of N_S [Fig. 1(c) $\theta = \theta_{\text{crit}} + 0.15 \text{ ML}$], which for these low growth rate conditions corresponds to $\sim 7 \times 10^{10} \text{ cm}^{-2}$. As the coverage is increased further, any extra material is added to existing QD's only, and no new nucleation processes occur. N_S remains constant, with only V increasing proportionally to the InAs coverage [Fig. 1(d), $\theta = \theta_{\text{crit}} + 0.70 \text{ ML}$].

Scaled 3D island size distributions for four different InAs coverages are shown in Fig. 2. Particular care was taken to ensure that *all* 3D surface features with $h > 6 \text{ \AA}$ were included in the data analysis, in contrast to the method used in Refs. 14, 15, and 20. The dimensions of the smallest features analyzed were $\sim 6 \text{ \AA} \times 60 \text{ \AA} \times 90 \text{ \AA}$ (height \times width \times length), and correspond to an island volume of ~ 400 atoms. More than 1850 QD's were used in the data analysis and the volumes were measured by directly integrating the STM intensity from several images using a customized image processing package. This approach makes no assumption about the shape of the QD's, which is still the subject of significant debate.²¹ The QD sizes are expressed as a number of "atoms," $s = V/V_0$, where V is the QD volume measured directly above the plane of the WL, and $V_0 = 27.8 \text{ \AA}^3$ is an estimate for the volume of one atom, assuming pure InAs composition for all QD's (a reasonable assumption given the

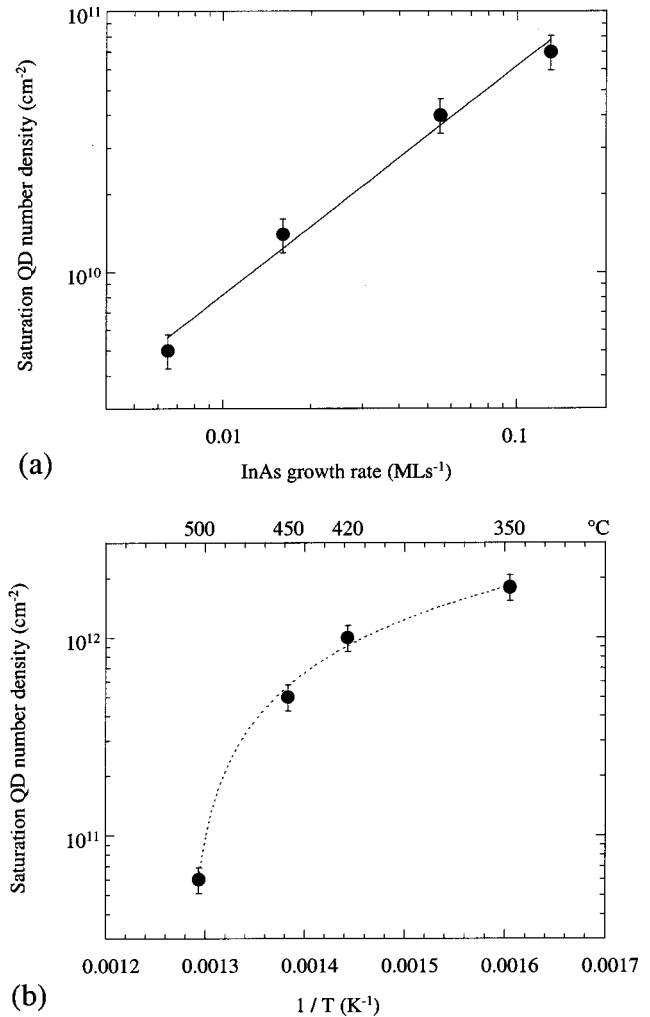


FIG. 3. A plot of the saturation QD number density as a function of (a) InAs growth rate (at a fixed substrate temperature of 500°C), and (b) inverse temperature (at a fixed InAs growth rate of 0.13 ML s^{-1}).

low growth rates used¹⁷). The actual number of atoms will depend on the composition of each individual QD, but s will still be proportional to the number of atoms in the QD.

Initially [Fig. 2(a)] the scaling function closely resembles that observed for $i=0$,⁹ implying that in adatoms freeze spontaneously on the surface immediately after deposition. At slightly higher coverages [filled circles in Figs. 2(b) and 2(c)] the shape of the island distribution shows crossover behavior from an $i=0$ like curve to $i=1$ type behavior. For a coverage of 1.81 ML and beyond [filled circles in Fig. 2(d)], the scaled distributions fall onto a slightly modified $i=1$ curve, with a skew towards small island sizes ($s/\langle s \rangle < 1$).

There are very clear differences in behavior before and after QD number density saturation, in clear contrast to the results of Ebiko *et al.*^{14,15} These cannot be attributed to growth rate effects: the evolution of the shape of the scaled QD island distributions (not shown) grown at an InAs growth rate comparable to that used by Ebiko *et al.* (0.13 ML s^{-1}) is very similar to the results shown in Fig. 2 (InAs

growth rate of 0.017 ML s^{-1}). STM data scaled using the analysis methods of Ref. 14 and 15 are shown as empty circles²² in Figs. 2(b)–2(d). All 3D features with $h < 12 \text{ \AA}$ were excluded from the data sets and QD volumes were calculated using the formula $V = 0.5 \times \text{height} \times \text{base area}$. To account for AFM tip convolution, lateral QD dimensions were adjusted using a geometrical convolution factor for a spherical AFM tip of radius 600 \AA , with a constant 6 \AA (2 ML) correction to the QD height data to account for a surface oxide layer. The AFM distributions are narrower than those from the normal STM data, with the maxima much closer to $s/\langle s \rangle = 1$ and a shape which more closely resembles that of an ideal $i = 1$ scaling distribution. The data at 1.72 ML [empty circles in Fig. 2(b)] and 1.76 ML [empty circles in Fig. 2(c)] now fall onto the scaling curve, which implies that the scaling of the 3D island size distributions observed in this coverage region by Ebiko *et al.* is an artifact of their analysis process.

The dependence of the saturation 3D island number density (prior to coalescence) in the complete condensation regime has been shown by Venables *et al.* to vary as⁸

$$N_S \propto F^{i/(i+2.5)} \exp\left(\frac{E_a}{k_b T}\right), \quad (2)$$

where F is the flux, E_a is the activation energy for diffusion given by $(E_i - iE_d)/(i + 2.5)$, E_i is the binding energy of a critical nucleus size i , E_d the diffusion energy and k_b is Boltzmann's constant. Assuming i is independent of temperature, plots of N_S as a function of F and T can *in principle* provide values for i and E_a , and hence for E_d . Figure 3(a) shows a plot of the saturation QD N_S as a function of InAs growth rate at a fixed substrate temperature of $500 \text{ }^\circ\text{C}$. A least squares fit yields a value of $i = 18$ for the critical nucleus size. Clearly, $i \neq 1$ at this typical QD growth temperature, and calculation of E_d is not straightforward since E_i is not a

simple function of i . The variation of the saturation N_S as a function of inverse growth temperature (at a fixed rate of 0.13 ML s^{-1}) is shown in Fig. 3(b). This data was taken from our previous study reported in Ref. 16, and it shows clearly that for $T \leq 500 \text{ }^\circ\text{C}$, the critical nucleus size changes continuously with growth temperature. Temperature-dependent critical nucleus sizes have been frequently observed in heteroepitaxial metal-on-metal S-K growth systems.²³ In our studies, the saturation N_S value varies inversely with temperature—this disagreement between experimental results and existing theory implies that the complexity of the InAs/GaAs QD growth process significantly diminishes the usefulness of Eq. (2), and thus noticeably reduces the applicability of relatively simple growth concepts to the modeling of complicated surface growth processes.

In conclusion, we have used high-resolution rapid quench MBE-STM to investigate the initial stages of InAs/GaAs(001) QD formation. We show that in the very earliest stages of QD nucleation and growth, just after θ_{crit} , the QD size distributions do not exhibit scaling behavior, in contrast to previously published results. Such scaling behavior is only observed in the postnucleation regime, after saturation of the QD number density. Our results show that strain is a significant factor in determining the *initial* QD size distributions but plays no role after saturation of the QD number density. A large critical nucleus size ($i = 18$ at $500 \text{ }^\circ\text{C}$) and the variation of i with growth temperature contradict predictions from classic nucleation theory and emphasise the limitations of using simple models for calculation of surface diffusion and binding energies in this complicated semiconductor heteroepitaxial material system.

This work was supported by the EPSRC, UK, who also provided financial support for P.B.J. and T.J.K. G.R.B. is grateful to the Ramsay Memorial Trust for the provision of financial support, funded in part by VG Semicon Ltd. (UK).

*Fax: +44-20-7594-5801. Email address: t.jones@ic.ac.uk

¹D. Bimberg, M. Grundmann, and N. N. Ledentsov, *Quantum Dot Heterostructures* (Wiley, Chichester, 1999); L. Jacak, P. Hawrylak, and A. Wójs, *Quantum Dots* (Springer, New York, 1998).

²C. Priester and M. Lannoo, Phys. Rev. Lett. **75**, 93 (1995).

³Y. Chen and J. Washburn, Phys. Rev. Lett. **77**, 4046 (1996).

⁴A.-L. Barabasi, Appl. Phys. Lett. **70**, 2565 (1997).

⁵L. G. Wang *et al.*, Phys. Rev. B **62**, 1897 (2000).

⁶H. T. Dobbs, D. D. Vvedensky, and A. Zangwill, Phys. Rev. Lett. **79**, 897 (1997).

⁷C. Ratsch *et al.*, Surf. Sci. **293**, 123 (1993); C. Ratsch *et al.*, J. Phys. I **6**, 575 (1996).

⁸J. Venables, G. D. T. Spiller, and M. Hanbucken, Rep. Prog. Phys. **47**, 399 (1984).

⁹J. G. Amar and F. Family, Phys. Rev. Lett. **74**, 2066 (1995).

¹⁰V. Bressler-Hill *et al.*, Phys. Rev. Lett. **74**, 3209 (1995).

¹¹G. R. Bell *et al.*, Phys. Rev. B **61**, R10 551 (2000).

¹²T. J. Krzyzewski *et al.*, Surf. Sci. **482-485**, 891 (2001).

¹³T. J. Krzyzewski *et al.* (unpublished).

¹⁴Y. Ebiko *et al.*, Phys. Rev. Lett. **80**, 2650 (1998).

¹⁵Y. Ebiko *et al.*, Phys. Rev. B **60**, 8234 (1999).

¹⁶P. B. Joyce *et al.*, Phys. Rev. B **58**, R15 981 (1998).

¹⁷P. B. Joyce *et al.*, Phys. Rev. B **62**, 10 891 (2000).

¹⁸M. C. Bartelt and J. W. Evans, Phys. Rev. B **46**, 12 675 (1992).

¹⁹B. A. Joyce *et al.*, Jpn. J. Appl. Phys., Part 1 **36**, 4111 (1997).

²⁰Additional errors in Refs. 14 and 15 arise from the limited resolution and tip convolution problems associated with AFM, especially for the investigation of small ($h < 12 \text{ \AA}$) 3D surface features, possible changes in N_S due to temperature (and not coverage) variations across the sample surface, the strong possibility of significant postgrowth surface rearrangement during sample annealing due to poor quenching, and the lack of absolute coverage measurements *independent* of the QD number density.

²¹Y. Nabetani *et al.*, J. Appl. Phys. **76**, 347 (1994); Y. Hasegawa *et al.*, Appl. Phys. Lett. **72**, 2265 (1998).

²²Insufficient data remained for the data set at 1.68 ML [Fig. 2(a)] to obtain a scaled QD size distribution.

²³H. Brune *et al.*, Phys. Rev. B **60**, 5991 (1999).